Biomedical Optics EXPRESS

Bedside monitoring of patients with shock using a portable spatially-resolved near-infrared spectroscopy

Ting Li,[1,4,5] Meixue Duan,[1,4] Kai Li,[1] Guoqiang Yu,[2] and Zhengshang Ruan[3,6]

[1]*State Key Lab Elect Thin Film & Integrated Device and Department of Biomedical Engineering, University of Electronic Science & Technology of China, Chengdu 610054, China*
[2]*Department of Biomedical Engineering, University of Kentucky, Lexington, KY 40506-0108, USA*
[3]*Department of Anesthesiology and Surgical Intensive Care Unit, Xinhua Hospital, Shanghai 200092, China*
[4]*These authors contributed equally to this work*
[5]*liting@uestc.edu.cn*
[6]*jyzqa@aliyun.com*

Abstract: Clinical monitoring of shock mainly depends on blood-oxygen-indices obtained from invasive blood sample tests. The central internal jugular central vein oxygenation level ($ScvO_2$) has been considered as a gold standard indicator for shock prediction. We developed a noninvasive spatially-resolved near-infrared spectroscopy (SR-NIRS) to measure tissue blood oxygen saturation (StO_2) surrounding the region of taking blood sample for the $ScvO_2$ test in 25 patients with shock. StO_2 values were found to be highly correlated ($r = 0.84$, $p < 0.001$) with $ScvO_2$ levels and the concordance coefficient of 0.80 is high. The results suggest the potential of noninvasive SR-NIRS for bedside shock monitoring.

OCIS codes: (170.1470) Blood or tissue constituent monitoring; (300.0300) Spectroscopy.

References and links

1. M. C. Houston, "Pathophysiology of shock," Crit. Care Nurs. Clin. North Am. **2**(2), 143–149 (1990).
2. A. B. Peitzman, T. R. Billiar, B. G. Harbrecht, E. Kelly, A. O. Udekwu, and R. L. Simmons, "Hemorrhagic shock," Curr. Probl. Surg. **32**(11), 925–1002 (1995).
3. R. A. Pedowitz and S. R. Shackford, "Non-cavitary hemorrhage producing shock in trauma patients: incidence and severity," J. Trauma **29**(2), 219–222 (1989).
4. D. C. Elliott, "An evaluation of the end points of resuscitation," J. Am. Coll. Surg. **187**(5), 536–547 (1998).
5. D. De Backer, G. Ospina-Tascon, D. Salgado, R. Favory, J. Creteur, and J. L. Vincent, "Monitoring the microcirculation in the critically ill patient: current methods and future approaches," Intensive Care Med. **36**(11), 1813–1825 (2010).
6. R. M. Durham, K. Neunaber, J. E. Mazuski, M. J. Shapiro, and A. E. Baue, "The Use of Oxygen Consumption and Delivery as Endpoints for Resuscitation in Critically III Patients," J. Trauma **41**(1), 32–40 (1996).
7. S. M. Cohn, A. B. Nathens, F. A. Moore, P. Rhee, J. C. Puyana, E. E. Moore, and G. J. Beilman; StO2 in Trauma Patients Trial Investigators, "Tissue oxygen saturation predicts the development of organ dysfunction during traumatic shock resuscitation," J. Trauma **62**(1), 44–55 (2007).
8. R. P. Dellinger, M. M. Levy, A. Rhodes, D. Annane, H. Gerlach, S. M. Opal, J. E. Sevransky, C. L. Sprung, I. S. Douglas, R. Jaeschke, T. M. Osborn, M. E. Nunnally, S. R. Townsend, K. Reinhart, R. M. Kleinpell, D. C. Angus, C. S. Deutschman, F. R. Machado, G. D. Rubenfeld, S. Webb, R. J. Beale, J. L. Vincent, and R. Moreno; Surviving Sepsis Campaign Guidelines Committee including The Pediatric Subgroup, "Surviving Sepsis Campaign: international guidelines for management of severe sepsis and septic shock, 2012," Intensive Care Med. **39**(2), 165–228 (2013).
9. B. A. Crookes, S. M. Cohan, J. Amotegui, R. Manning, P. Li, M. S. Proctor, A. Hallal, Blackbourne, R. Benjamin, D. Soffer, F. Habib, C. I. Schulman, R. Duncan, and K. G. Proctor, "Can near-infrared spectroscopy identify the severity of shock in trauma patients?" J. Trauma Acute Care Surg. **58**(4), 806–816 (2005).
10. F. Torella, R. D. Cowley, M. S. Thorniley, and C. N. McCollum, "Regional tissue oxygenation during hemorrhage: can near infrared spectroscopy be used to monitor blood loss?" Shock **18**(5), 440–444 (2002).
11. B. A. McKinley, R. G. Marvin, C. S. Cocanour, and F. A. Moore, "Tissue hemoglobin O2 saturation during resuscitation of traumatic shock monitored using near infrared spectrometry," J. Trauma **48**(4), 637–642 (2000).
12. M. M. Knudson, K. M. Bermudez, C. A. Doyle, R. C. Mackersie, H. W. Hopf, and D. Morabito, "Use of tissue oxygen tension measurements during resuscitation from hemorrhagic shock," J. Trauma **42**(4), 608–616 (1997).

#242023 Received 1 Jun 2015; revised 8 Jul 2015; accepted 8 Jul 2015; published 19 Aug 2015

13. G. J. Beilman, K. E. Groehler, V. Lazaron, and J. P. Ortner, "Near-infrared spectroscopy measurement of regional tissue oxyhemoglobin saturation during hemorrhagic shock," Shock **12**(3), 196–200 (1999).
14. M. Lipcsey, N. C. Z. Woinarski, and R. Bellomo, "Near infrared spectroscopy (NIRS) of the thenar eminence in anesthesia and intensive care," Ann. Intensive Care **2**(1), 11 (2012).
15. K. Waxman, C. Annas, K. Daughters, G. T. Tominaga, and G. Scannell, "A method to determine the adequacy of resuscitation using tissue oxygen monitoring," J. Trauma **36**(6), 852–858 (1994).
16. T. Li, Y. Zhao, K. Li, Z. Ruan, M. Duan, and Y. Sun, "Study on shock monitoring using a space-resolved NIRS," PIBM 2014, Proc. SPIE. in press.
17. S. Hyttel-Sorensen, L. C. Sorensen, J. Riera, and G. Greisen, "Tissue oximetry: a comparison of mean values of regional tissue saturation, reproducibility and dynamic range of four NIRS-instruments on the human forearm," Biomed. Opt. Express **2**(11), 3047–3057 (2011).
18. C. Jenny, M. Biallas, I. Trajkovic, J. C. Fauchère, H. U. Bucher, and M. Wolf, "Reproducibility of cerebral tissue oxygen saturation measurements by near-infrared spectroscopy in newborn infants," J. Biomed. Opt. **16**(9), 097004 (2011).
19. T. Li, H. Gong, and Q. Luo, "MCVM: Monte Carlo modeling of photon migration in voxelized media," J. Innov. Opt. Health Sci. **3**(2), 91–102 (2010).
20. T. Li, H. Gong, and Q. Luo, "Visualization of light propagation in visible Chinese human head for functional near-infrared spectroscopy," J. Biomed. Opt. **16**(4), 045001 (2011).
21. D. Boas, J. Culver, J. Stott, and A. Dunn, "Three dimensional Monte Carlo code for photon migration through complex heterogeneous media including the adult human head," Opt. Express **10**(3), 159–170 (2002).
22. S. Fantini, D. Hueber, M. A. Franceschini, E. Gratton, W. Rosenfeld, P. G. Stubblefield, D. Maulik, and M. R. Stankovic, "Non-invasive optical monitoring of the newborn piglet brain using continuous-wave and frequency-domain spectroscopy," Phys. Med. Biol. **44**(6), 1543–1563 (1999).
23. H. Liu, D. A. Boas, Y. Zhang, A. G. Yodh, and B. Chance, "Determination of optical properties and blood oxygenation in tissue using continuous NIR light," Phys. Med. Biol. **40**(11), 1983–1993 (1995).
24. L. I. Lin, "A concordance correlation coefficient to evaluate reproducibility," Biometrics **45**(1), 255–268 (1989).

1. Introduction

Shock may result in an acute blood flow reduction, metabolic abnormalities, anaerobic metabolism, cellular and organ dysfunction, and irreversible damage and death if prolonged [1]. The shock resulting from inevitable hemorrhage during surgery and traumatic injury is a fatal complication (up to 50% in mortality), frequently leading to early deaths [2,3]. Estimation of shock severity is crucial to guide clinicians for making treatment plans and for evaluating therapeutic effects [4].

The widely used clinical method to determine shock severity is to measure blood sample oxygen indices. Various oxygen-related indices were proposed as shock indicators, such as oxygen delivery (DO_2), oxygen consumption (VO_2), blood lactate, pulse oxygen saturation (SpO_2), central venous oxygen saturation ($ScvO_2$), artery oxygen saturation (SaO_2), and partial pressure of oxygen (PO_2). Among these indicators, only SpO_2 can be detected noninvasively by a finger-sensor. However, finger pulse oximetry works ineffectively during shock because of the poor peripheral blood perfusion in the finger [5]. The global indicators of DO_2 and VO_2 may not catch up regional hypoperfusion [6]. Blood lactate is not sensitive to pre-existing medical conditions [7]. PO_2 has been used for monitoring shock in an uncontrolled study with a small number of patients [4]. $ScvO_2$ [8] and SaO_2 are accepted to be accurate and objective for shock monitoring [9], and $ScvO_2$ is commonly regarded as a gold standard [8]. However, the invasive and intermittent procedures to obtain these acceptable indicators (i.e., PO_2, $ScvO_2$, SaO_2) limit the use for continuous shock monitoring. As a result, the clinician may miss the best time window to rescue the patient. Therefore, it's crucial to explore a noninvasive technique to continuously monitor shock.

Near-infrared spectroscopy (NIRS) permits noninvasive and continuous measurements of tissue blood oxygenation. The NIRS devices are usually portable, permitting bedside monitoring. There have been recently exploratory studies using NIRS for shock monitor [4, 9–15]. Some of them were carried out on animal models [12,13] or healthy human subjects [14]. A few were performed in patients either invasively with optical sensors inserted into subcutaneous and intramuscular sites [4,15] or noninvasively with optical probes placed on the peripheral muscles [9–11]. However, shock usually results in a poor peripheral blood circulation [5], leading to an insensitive measurement.

#242023 Received 1 Jun 2015; revised 8 Jul 2015; accepted 8 Jul 2015; published 19 Aug 2015

Shock occurs mostly because of insufficient blood oxygen to the body. Tissue blood oxygen saturation (StO_2) measured at an appropriate region may be a good indicator of shock state [9–11]. In this study, we investigated the correlations between StO_2 and $ScvO_2$, SaO_2, and PO_2, and explored the use of StO_2 as an indicator for shock.

2. Methods and materials

2.1. Spatially-resolved NIRS

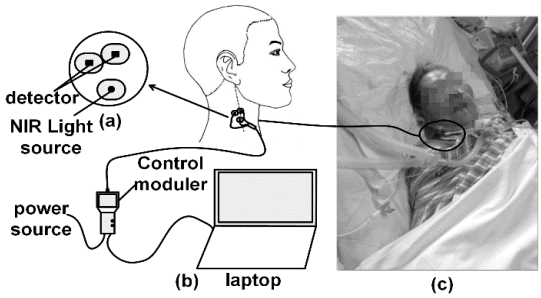

Fig. 1. Portable spatially-resolved near-infrared spectroscopy (SR-NIRS) device for bedside shock monitoring. (a) SR-NIRS probe placement; (b) SR-NIRS shock monitor device; (c) Bedside shock monitoring.

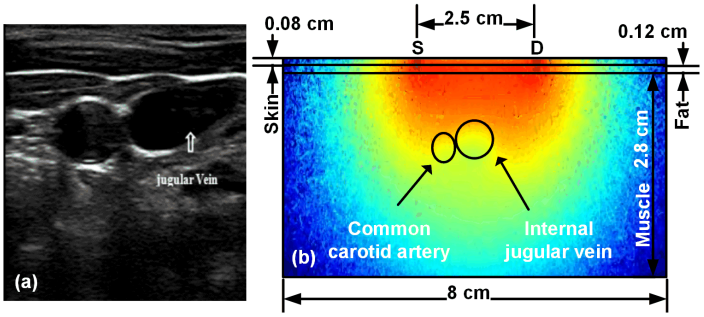

Fig. 2. (a) Ultrasonograph of internal jugular central vein and (b) Monte Carlo simulation of photon paths within the tissues surrounding the veins.

We have developed a SR-NIRS to monitor StO_2 in the region surrounding the internal jugular vein [16]. Two detectors and a 3-wavelengths (735, 805, and 850 nm) integrated LED were integrated into a probe (Fig. 1(a)) [17,18]. The LED was controlled by a micro-controller to be "on" or "off" alternatively. Relatively larger source-detector distances (2.4 cm and 2.7 cm) were used to probe deeper tissue property around the internal jugular vein, which located ~1 cm beneath the skin/probe (Fig. 1(b), 1(c), Fig. 2), and thus yielding more sensitive signals for the comparison of StO_2 and $ScVO_2$ measurements. The diameter of each detector was ~0.6 cm, making it impossible to arrange S-Ds in a linear pattern. Thus they were configured in a shape of triangle. Figure 2(b) shows Monte Carlo Simulation [19–21] of NIRS signal sensitivity profile with our probe design, suggesting that the sampling volume of our probe covered the tissue surrounding the central internal jugular vein. The size and depth of the veins in shock patients were determined by ultrasonographs. The thicknesses of skin and fat over the measured population were 0.2 ± 0.04 cm (mean ± standard deviation) measured by a Vernier caliper.

The calculation of local StO_2 was accomplished by converting from the detected light intensity changes based on the modified Beer-Lambert law [22,23]. The following formula describes the relationship between the measured optical density (OD), tissue optical properties, and the source-detector spacing (ρ):

#242023 Received 1 Jun 2015; revised 8 Jul 2015; accepted 8 Jul 2015; published 19 Aug 2015

$$OD = \log\left[\frac{R_{app0}(\rho,\rho_0)}{R_{app}(\rho,\rho_0)}\right] = \frac{\mu_{eff} - \mu_{eff}(cal)}{2.3}\rho + \log\left[\frac{\mu_t'}{\mu_t'(cal)}\right] + \log\left[\frac{\mu_{eff}(cal) + (1/\rho_0)}{\mu_{eff} + (1/\rho_0)}\right] \quad (1)$$

Here, ρ_0 is the average of the chosen maximum and minimum source-detector separations in the probe, R_{app} is the spatial dependence of the approximated diffuse reflectance, and $\mu_{eff} = \sqrt{3\mu_a(\mu_a + \mu_s(1-g))}$. μ_a is the absorption coefficient, μ_s is the scattering coefficient, and g is the anisotropic factor. *cal* means the calibration control. We then plotted *OD* changes as a function of ρ and the $slope_{\lambda i}$ of the plotted curve was calculated. The correlation between $slope_{\lambda i}$ and $\mu_{a\lambda i}$ was calculated as follows:

$$\frac{slope_{\lambda_1}}{slope_{\lambda_2}} = \frac{\mu_{eff\,\lambda_1}}{\mu_{eff\,\lambda_2}} = \sqrt{\frac{3\mu_{a\lambda_1}(\mu_{a\lambda_1} + \mu_{s\lambda_1}(1-g))}{3\mu_{a\lambda_2}\mu_{s\lambda_1}(1-g)}} \approx \sqrt{\frac{\mu_{a\lambda_1}}{\mu_{a\lambda_2}}} \quad (2)$$

The relationship between μ_a and the concentrations of deoxy-hemoglobin (Hb) and oxy-hemoglobin (HbO_2) can be described as follows:

$$\begin{cases} \mu_{a\lambda_1} = \varepsilon_{Hb\lambda_1}[Hb] + \varepsilon_{HbO_2\lambda_1}[HbO_2] \\ \mu_{a\lambda_2} = \varepsilon_{Hb\lambda_2}[Hb] + \varepsilon_{HbO_2\lambda_2}[HbO_2] \end{cases} \quad (3)$$

Here, $\varepsilon_{Hb\lambda i}$ and $\varepsilon_{HbO_2\lambda_1}$ represents the extinction coefficient of Hb and HbO_2 respectively. The mathematical definition of StO_2 is given by:

$$StO_2 = \frac{[HbO_2]}{[HbO_2 + Hb]} \times 100\% \quad (4)$$

By substituting Eqs. (3) and (4) into Eq. (2), StO_2 was obtained as follows:

$$StO_2 = \frac{\varepsilon_{Hb\lambda_2} slope_{\lambda_1}^{\,2} - \varepsilon_{Hb\lambda_1} slope_{\lambda_2}^{\,2}}{\varepsilon_{Hb\lambda_2} slope_{\lambda_1}^{\,2} - \varepsilon_{Hb\lambda_1} slope_{\lambda_2}^{\,2} + \varepsilon_{HbO_2\lambda_1} slope_{\lambda_2}^{\,2} - \varepsilon_{HbO_2\lambda_2} slope_{\lambda_1}^{\,2}} \times 100\% \quad (5)$$

2.2 Subjects and experimental protocol

Twenty-five patients with shock were recruited from Xinhua Hospital in Shanghai of China with their written informed consents approved by the ethics committee (Approval No. XHEC-D-2014-005). Patients were 67.3 ± 16.6 years old. StO_2 measurements were performed using our SR-NIRS device in conjunction with other conventional shock monitoring procedures. The StO_2 measurements were carried out either at the end of shock treatment (8 males and 5 females) or one day after (7 males and 5 females). The internal jugular central venous catheterization could not be performed on the former group of patients since the measurement site was still occupied to perform tracheal intubation to obtain respiration-oxygen delivery at that point.

2.3 Data collection and analysis

We used the ultrasound to locate the internal jugular central vein and to aid the placement of SR-NIRS probe (see Fig. 2(a), Fig. 1(b), 1(c)). The probe position was fine-tuned and fixed until the signal became stable. After collecting SR-NIRS data for 5 minutes, blood sampling through the central venous catheter was performed to obtain the indices of $ScvO_2$, SaO_2, and PO_2. We also collected SpO_2 data from finger sensor.

All data analysis was performed with MATLAB R2010b, MathWorks, USA. Statistical significance was declared for p values < 0.05. We performed correlation analysis of StO_2 with $ScvO_2$, PO_2, and SaO_2 respectively and reported the Pearson' correlation coefficient r, which ranged from 0 to 1 to estimate linear correlation extent. To quantify the relationship of StO_2

#242023 Received 1 Jun 2015; revised 8 Jul 2015; accepted 8 Jul 2015; published 19 Aug 2015

with combinations of the acceptable blood oxygen indices, we fit multiple linear regression models. We also test the consistency between StO_2 and $ScvO_2$ and reported Lin's concordance coefficient [24], which combines a measure of precision and accuracy. A Bland-Altman plot was carried out to visualize the extent of agreement between the indicators.

3. Results

SpO_2 measurements were not reliable on our patients with shock; almost all showed low invalid values or no readout except one patient had a value 95% which was in the valid range.

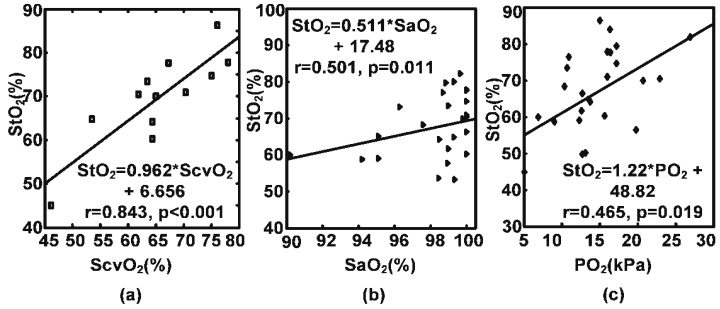

Fig. 3. The correlations between StO_2 and conventional blood oxygen indices, represented by scatter plot with least-squares fitted lines added.

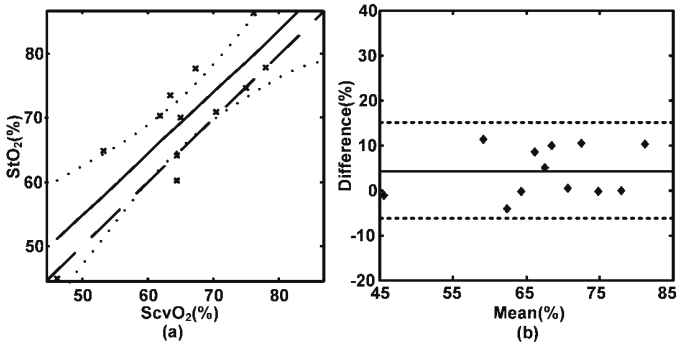

Fig. 4. NIRS-measured StO_2 compared to the gold standard $ScvO_2$ from the blood sample test. (a) The solid line represents the best fit to the data; the dashed line indicates the perfect equivalent; and the dot line denotes the 95% confidence interval for StO_2. (b) Bland-Altman plot of the deference between the StO_2 and $ScvO_2$ as well as the mean difference (solid horizontal line) between these two parameters. The dash lines indicate the 95% limits of an agreement.

The comparisons between the StO_2 measured by SR-NIRS and other shock-monitoring clinical measures are shown in Fig. 3, 4 and Table 1. A significant linear relationship was observed ($r > 0.843$, $p < 0.001$) between the StO_2 and $ScvO_2$ (see Fig. 3(a)), with a slope (95% confidence interval) of 0.96 (0.53 to 1.39) (see Fig. 4(a)). Only three data points fell outside 95% confidence level. The Bland-Altman plot (Fig. 4(b)) for these two measurements also demonstrated an agreement, with a mean difference of 4.16% (−6.87% to 15.20%). The concordance coefficient between StO_2 and $ScvO_2$ of 0.804 is high. Additionally, StO_2 was found to be correlated with SaO_2 ($r = 0.501$, $p = 0.011$; see Fig. 3(b)) and PO_2 ($r = 0.465$, $p = 0.019$; see Fig. 3(c)) and there were significant regressions between StO_2 and other acceptable blood oxygen indices (Table 1). The corresponding residual analysis showed only two patients had outlier data, also indicating the robust regression relationships.

#242023 Received 1 Jun 2015; revised 8 Jul 2015; accepted 8 Jul 2015; published 19 Aug 2015

Table 1. Multiple linear regression analysis (MLR) of StO_2 with conventional blood oxygen indices

Combination	r	p
StO_2 (PO_2, SaO_2)	0.56	0.017*
StO_2 (PO_2, $ScvO_2$)	0.82	0.0045**
StO_2 (SaO_2, $ScvO_2$)	0.81	0.0013**

*$p < 0.05$; **$p < 0.01$.

There were no significant differences in StO_2, SaO_2 and PO_2 between the measures at different days (i.e., the day at treatment versus one day after treatment) ($p > 0.16$), hence it is not unreasonable to speculate that $ScvO_2$ might show obscure difference as well. It may contribute to the effective resuscitation on the shocks.

4. Discussion and conclusion

Continuous monitoring of shock is crucial for clinicians to perform treatment timely and evaluate therapeutic effect so that irreversible injuries can be avoided. However, currently available methodologies for shock monitoring rely on frequent blood sampling with internal jugular central venous catheterization, which is invasive and discontinuous. In this study, we demonstrated that the StO_2 level measured at the tissues surrounding the internal jugular vein by noninvasive SR-NIRS may be a shock indicator. The SR-NIRS used in this study enabled absolute measurement of StO_2. Data from 25 patients with shock demonstrate significant correlations between StO_2 and the gold standard $ScvO_2$ as well as other acceptable blood oxygen indices. These results support the use of SR-NIRS as a noninvasive, continuous tool for bedside monitoring of shock.

Our study is the first exploration of the StO_2 measured by NIRS at the region surrounding the internal jugular central vein as a new shock indicator. Previous studies using NIRS to monitor StO_2 in shocks were performed in the peripheral area including finger, deltoid muscle, subcutaneous tissue, and thenar eminence [11,13]. However, shock usually results in poor peripheral blood circulation, making peripheral measurements unreliable, as seen in this study with SpO_2 measurements. By contrast, we chose the tissue surrounding internal jugular central veins because the gold standard $ScvO_2$ sampling is usually taken from this vein [11] and this site roughly belongs to splanchnic circulation which is crucial for shock monitoring. We may also explore other potential sites such as patient's head in the future as cerebral circulation is apparently critical for shock monitoring.

The StO_2 measured by NIRS showed strong correlation and high concordance with the gold standard $ScvO_2$, which might be because a portion of the signal $ScvO_2$ goes into the StO_2 (see Fig. 2(b)) measured in the tissue surrounding the internal jugular central vein. Meanwhile, the StO_2 showed weak correlations with other indicators (i.e., SaO_2 and PO_2), indicating that the StO_2 measurement performed closer to the vein for the $ScvO_2$ test is supper than other places for monitoring shock states. However, the thresholds to separate healthy subjects and shock patients using $ScvO_2$ and StO_2 have not been established yet, and further investigations including healthy subjects are needed.

In summary, we have demonstrated that NIRS measurements of StO_2 in the internal jugular central venous region provide valuable information for shock monitoring. The NIRS-measured StO_2 has been verified by comparing to the conventional blood oxygen indices, especially $ScvO_2$. SR-NIRS device can be used at the bedside for continuous monitoring of shock, and thus has the potential to become a clinical tool for shock management.

#242023 Received 1 Jun 2015; revised 8 Jul 2015; accepted 8 Jul 2015; published 19 Aug 2015